IEEE Access
Multidisciplinary | Rapid Review | Open Access Journal

Received April 12, 2019, accepted May 1, 2019, date of publication May 13, 2019, date of current version May 30, 2019.

Digital Object Identifier 10.1109/ACCESS.2019.2916412

Robust QFT-Based Feedback Linearization Controller of the Greenhouse Diurnal Temperature Using Natural Ventilation

A. HOYO, J. C. MORENO, J. L. GUZMÁN, AND F. RODRÍGUEZ

CIESOL Research Center on Solar Energy, Informatics Department, Agrifood Campus of International Excellence CeiA3, University of Almería, 04120 Almería, Spain

Corresponding author: J. L. Guzmán (joseluis.guzman@ual.es)

This work was supported in part by the DPI2017-85007-R through the Spanish Ministry of Science and Innovation, and in part by the EU-ERDF Funds.

ABSTRACT In this paper, a control scheme based on feedback linearization technique and quantitative feedback theory (QFT) is used to regulate the inner diurnal temperature in a greenhouse located in the south of Spain. In a first step, a non-linear model for the greenhouse is used to design a feedback linearization controller, which provides the vents opening percentage from a virtual control signal provided by a robust proportional integral (PI) controller. The relation between the system output (inside temperature of the greenhouse) and the virtual control signal is given by a first order plus dead time (FOPDT) system. The values for the three parameters of this linear model are identified in the experimental greenhouse by applying several step changes in the virtual control signal and analyzing the process response. Different values for gain, the time constant, and time delay are identified. So, this uncertain linear description for the system is used to design a quantitative feedback theory (QFT) controller with a PI structure. Finally, experimental results are analyzed showing satisfactory performance of the proposed control approach.

INDEX TERMS Climate control, feedback linearization, greenhouse, quantitative feedback theory.

I. INTRODUCTION

The main objective of greenhouses is to increase the economic benefits of the farmer looking for a tradeoff between incomes, the cost of obtaining the optimal climate conditions for the crop growth, and the fulfillment of the regulations on agriculture and environment. These regulations are often based on obtaining a product suitable for human consumption, avoiding pollution, and minimizing the impact on the environment. Automatic control strategies are a solution to allow farmers meeting these objectives.

The microclimate provided by a greenhouse allows to obtain crop production in seasons where it would not be possible to produce with open systems. Furthermore, crop growth needs suitable environmental conditions to maximize its production. So, it is important to keep climatic variables inside the greenhouse in optimal conditions, specially temperature and humidity. This can be achieved using automatic control techniques. Therefore, over the years, the scientific community has been actively working on the modelling and control of greenhouses, trying to optimize the use of resources (water, energy, human worker hours,...), while minimizing the effects on the environment. A survey about greenhouse climate control is presented in [1]. In [2], for example, a hierarchical architecture is proposed where the lower layer consists of a linear quadratic optimal controller based on an linearized model for the greenhouse temperature. In this case, a heating system is used as control actuator. However, the standard tool to obtain the necessary environmental conditions is the regulation of the natural ventilation of the greenhouse. In [3], a PSO-based MPC is used to control the temperature of a greenhouse using forced heating and natural ventilation. In [4], a Bayesian is implemented to control the greenhouse indoor temperature, acting directly on the ventilation. This network learns from previous manual and automatic control actions for predefined setpoints in presence of changing outer environmental conditions. In [5], a two time-scales receding horizon optimal control system is implemented, where forced heating, CO_2 supply, ventilation system, and LED lighting are used to achieve the crop growth

The associate editor coordinating the review of this manuscript and approving it for publication was Mohsin Jamil.

objectives. In [6], Symmetric Send-On-Delta event based PI controllers are applied to control the inside air temperature using natural ventilation, and in [7] the greenhouse temperature is controlled using natural ventilation by means of a non-linear model predictive control strategy. The controller is based on a second-order Volterra series model obtained from experimental data. In [8], a multiobjective hierarchical control architecture is proposed for greenhouse crop growth problem. Therefore, a wide variety of control strategies have been proposed and used for the greenhouse climate control problem.

The control problem difficulty resides in the complexity of the greenhouse model. Its behavior is described in terms of a set of non-linear differential equations including mass balances and energy transfer in the plastic cover, soil surface, one soil layer, and crop. These processes depend on the outside environmental conditions, greenhouse structure, type and state of the crop, and on the effect of the control actuators [9]. For designing the controller, and in order to deal with the greenhouse non-linearities, some classical methodologies based on non-linear control theory have been used. The feedback linearization control law [10] is a clear example. In [11], a model-based approach is combined with feedback linearization to cope with the external disturbances, taking the constrains of the actuators into account to define feasible setpoints. A PI feedback controller is used to cope with the uncertain of the process but in an implicit form, without explicitly considering the uncertainty in the design process. In [12], an adaptive feedback linearization with predictive control is proposed, and in [13] a non-linear model predictive control via feedback linearization is also developed, to control in both cases the inside temperature.

Classical feedback linearization control strategies rely on detailed system models and on the hypothesis that perfect dynamics cancellation is achieved. However, the modelling errors are always presented and thus perfect cancellation is not realizable. So, model uncertainties should be considered when the feedback linearization approach is combined with other control strategy. Notice that robust control techniques have been applied to the greenhouses climate control problem considering the uncertainties directly on the model, but without using the feedback linearization technique. For instance, in [14], a robust control algorithm based on the Quantitative Feedback Theory (QFT) and feedforward control is used to achieve adequate values of inside greenhouse temperature in spite of uncertainties and disturbances acting on the system.

In this work, the feedback linearization control technique is used in combination with QFT to control the greenhouse inside temperature. This combination allows to cope with the complex non-linear climate control problem and to account for model uncertainties. First, the feedback linearization approach was implemented in the real system, and open-loop tests were performed on the virtual control signal. Then, from these experiments, a linear model was obtained with uncertain parameters due to physical parameters variability and the disturbances effect. So, the QFT approach was used to design a robust controller to compensate for the process uncertainties on the resulting approximated linear model. Therefore, as a result, the combined control approach FL+QFT was implemented to control the greenhouse inside temperature in spite of non-linearities, uncertainties, and disturbances. The proposed control architecture was evaluated through real experiments with different environment conditions and promising results were obtained. For that reason, comparisons with other control strategies were not considered since it is impossible to evaluate and compare them under the same operation conditions.

The paper is organized as follows. In section II, the system is described, where the greenhouse process and the climate control problem are presented. Then, in section III the proposed robust non-linear control is summarized. In section IV, the experimental results are shown. Finally, section V presents the manuscript conclusions.

II. SYSTEM DESCRIPTION

In this section, the greenhouse where the experiments are performed is described. The structure, sensors and actuators of the system, together with the climate problem are detailed.

A. THE GREENHOUSE

Experiments were carried out in a parral greenhouse located at The Cajamar Foundation (El Ejido, Almería, South-East Spain) (Figure 1). The material that covers the greenhouse is a PE film of 200 μm thickness, installed on a galvanized steel structure. The actuators are a hinged roof window with a maximum opening angle of 45°, and a lateral window with a length of 37 m and an opening from 0° to 45°. The greenhouse has a great variety of sensors to obtain data. Soil temperature is measured using semiconductor sensors at different depths (just below the surface layer of the soil and 50 mm deep) and on both sides of the mulch. To measure the outside temperature eight semiconductor contact sensors have been installed along the cover. The temperature of the air and the relative humidity inside the greenhouse are measured by means of thermoresistive and capacitive sensors, respectively, positioned in the upper part of the crop. Outside the greenhouse a meteorological station has been installed at a height of 6 m to measure temperature, relative humidity, global radiation, photosynthetic radiation (PAR), rain, and wind speed and direction.

B. CLIMATE PROBLEM

The structure of the greenhouse, the type and state of the crop, the effect of the actuators and the outlet environmental conditions affect the dynamic behavior of the greenhouse inside climate (see Figure 2).

All the processes that happen inside and outside the greenhouse have a strong relationship between them. The inside diurnal temperature varies by convective air exchange between the outside and inside [15]. This exchange rate coupled with CO_2 taken by the crop during photosynthesis

FIGURE 1. Greenhouse facilities used for the experiences performed in this work.

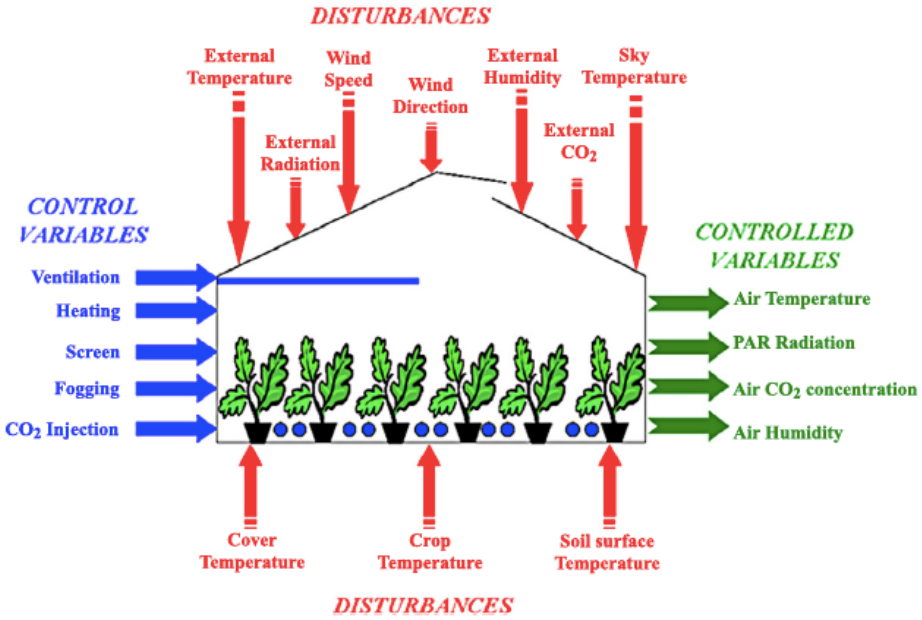

FIGURE 2. Greenhouse climate control problem.

determine the concentration of CO_2 in the greenhouse. When the photosynthetic rates are higher, the concentration of CO_2 falls below the atmospheric, producing a growth deficit that is increased when the crop reaches its maximum development [9]. Furthermore, photosynthesis rate indirectly affects the humidity content because when the leaves stomata are opened to capture the CO_2, the plant emits water vapor through the transpiration process increasing the humidity inside the greenhouse. This released vapor can be reduced and the concentration of CO_2 increased by ventilation [16].

Inside the greenhouse, the crop growth is influenced by PAR radiation, temperature, and CO_2 level. Under diurnal conditions, PAR radiation and temperature influence the process of plant photosynthesis. In particular, temperature

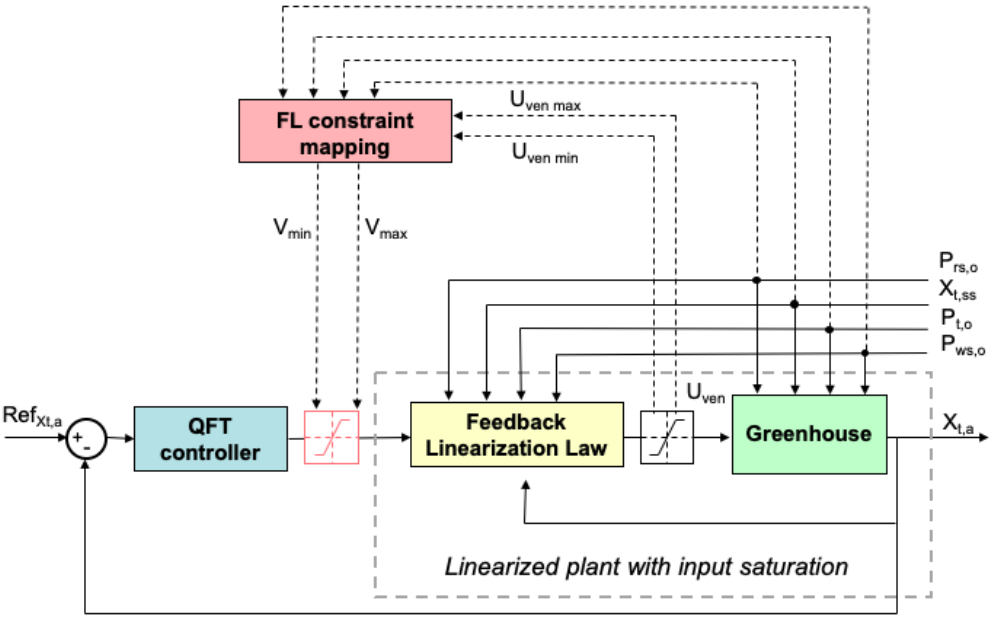

FIGURE 3. Proposed control scheme.

influences the speed of sugar production by photosynthesis and a higher radiation level implies a higher temperature. Thus, radiation and temperature have to be in balance and it is necessary to maintain the temperature in a level optimal for the photosynthesis process. The diurnal temperature control problem is the refrigeration of the greenhouse air using natural ventilation to reach the optimal temperature. The air exchange and flow inside the greenhouse is determined by natural ventilation as a consequence of the difference between inside and outside temperatures. The objective of the control system is to maintain the inside temperature close to an optimal level [9], having a direct effect on the crop growth.

III. ROBUST NON-LINEAR CONTROLLER

In this section, the calculation of the controller is developed combining FL and QFT control techniques. Due to the strong non-linearity and complexity of the system, FL is used first to simplify the controller design. So, a linearized FOPDT (First Order Plus Dead Time) model of the plant can be obtained from the combination of FL with the real process. This linear FOPDT model is calibrated by making tests on the real plant, where the FL non-linear block is placed in series with the greenhouse. Notice that due to the modelling errors and variability of the process disturbances, an uncertain FOPDT model is obtained. Then, for this reason, QFT is used to design a robust controller to control the combination of FL and the greenhouse. Figure 3 shows the control scheme implemented in the real system, and that will be described in detail in this section.

A. MODELLING AND FEEDBACK LINEARIZATION

This section summarizes the greenhouse non-linear model used in this work and its combination with the FL technique. Table 1 shows all the variables used in the equations for the non-linear model of greenhouse [9].

In order to describe the indoor climate greenhouse model, the following hypothesis are assumed:

- The state variable for the system is the air temperature, $X_{t,a}$, and it is considered also as the controlled variable.
- There are three external elements that interact with the greenhouse: outside air, floor surface and the crop.
- Exogenous variables and disturbances affecting the system and considered as environmental conditions are the outdoor air temperature, $P_{t,o}$, wind speed $P_{ws,o}$, outdoor global radiation, $P_{rs,o}$ and ground surface temperature, $X_{t,ss}$.
- System control input is ventilation position U_{ven}.
- Air is not inert to solar radiation.
- There is not reflection.
- Air physical characteristics, as density or specific heat, are constant with temperature and time.

Thus, according to the previous statements, the accumulated heat on the greenhouse air is given by the following balance equation [9]. Notice that references to t variable have been deleted in equations in order to obtain more compact expressions (see Table 1):

$$Q_{ac} = Q_s + Q_{cv,ss} + Q_{cv,cal} - Q_{cn-cv} - Q_v - Q_{t,c} \quad (1)$$

where Q_{ac} is the accumulated heat in the greenhouse air, Q_s is the solar radiation absorbed by the greenhouse air, $Q_{cv,ss}$ is the heat transfer by convection and conduction in the cover between the outside and the inside air, $Q_{cv,cal}$ is the convection heat transfer with the pipes heating system, Q_{cn-cv} is the convection and conduction heat transfer between the input and output greenhouse air, Q_v is the heat transfer to the

TABLE 1. Constants and variables.

$C_{a,s}$	Soil surface area (m^2)
C_{aoc}	Greenhouses air's short wave absorption coefficient (-)
C_{cv}	Greenhouse air-soil surface convection coefficient ($Wm^{-2}K^{-1}$)
C_{cn-cv}	Conduction and convection in the cover heat coeffient ($Wm^{-2}K^{-1}$)
$C_{d,a}$	Air density ($Kg\ m^{-3}$)
C_{et}	Evapotranspiration constant ($J\ kg^{-1}$)
C_f	Conversion factor ($J\ kg^{-1}K^{-1}$)
C_g	Gravity constant (ms^{-2})
$C_{sh,a}$	Air specific heat ($J\ kg^{-1}K^{-1}$)
$C_{v,d}$	Ventilation discharge coefficient (-)
$C_{v,l-l}$	Length of lateral vents (m)
$C_{v,l-r}$	Length of roof vents (m)
$C_{v,s}$	Air volume inside the greenhouse (m^3)
$C_{v,w-l}$	Width of lateral vents (m)
$C_{v,w-r}$	Width of roof vents (m)
$C_{ven,h}$	Ventilation effective height (m)
$C_{ven,w}$	Ventilation wind effect coefficient (-)
E_t	Evapotranspiration ($Kgs^{-1}m^{-2}$)
ϕ_l	Leakage by infiltration when vents are closed flux (m^3s^{-1})
$\phi_v(t)$	Ventilation flow (m^3s^{-1})
n_l	Number of lateral vents (-)
n_r	Number of roof vents (-)
$P_{rs,o}(t)$	Outside solar radiation (Wm^{-2})
$P_{t,o}(t)$	Outside temperature (K)
$P_{ws,o}(t)$	Wind speed ($m\ s^{-1}$)
Q_{ac}	Accumulated heat in the greenhouse air (Wm^{-2})
Q_s	Solar radiation absorbed by the greenhouse air (Wm^{-2})
$Q_{cv,ss}$	Ground surface convection heat transfer (Wm^{-2})
$Q_{cv,cal}$	Convection heat transfer with the pipes heating system (Wm^{-2})
Q_{cn-cv}	Heat transfer by convection and conduction in the cover between the outside and the inside air (Wm^{-2})
Q_v	Input and output exchange due to natural ventilation (Wm^{-2})
$Q_{t,c}$	Latent heating produced by the crop transpiration (Wm^{-2})
$U_{ven}(t)$	Vent opening control signal (^{o})
$V_{v,a-l}$	Areas of the roof ventilation openings (m^2)
$V_{v,a-r}$	Areas of the sidewall ventilation openings (m^2)
$V_{t,c}$	Short wave transmission coefficient based on the cover transmission coefficient, it whitening and the shader mesh state (-)
$X_{t,a}(t)$	Air temperature (K)
$X_{t,ss}(t)$	Soil surface temperature (K)

outside air due to ventilation and infiltration losses, and $Q_{t,c}$ is the latent heating produced by the crop transpiration.

Expressing the accumulated heat in the greenhouse as the variation of inside air temperature $X_{t,a}$ with respect to time, it results that:

$$C_{sh,a}C_{d,a}\frac{C_{v,s}}{C_{a,s}}\frac{dX_{t,a}}{dt} = Q_s + Q_{cv,ss} - Q_{cn-cv} - Q_v - Q_{t,c} \quad (2)$$

where $C_{sh,a}$ is the air specific heat, $C_{d,a}$ is air density, $C_{v,s}$ is air volume, $C_{a,s}$ is the surface ground area, and where $Q_{cv,cal}$ is zero due to the heating system is turned off.

Then, according to the results obtained in [9] for the balances presented in (2), and considering that in this paper only the diurnal dynamics is considered ($Q_{cv,cal} = 0$), the following greenhouse temperature simplified model is obtained:

$$\begin{aligned} &C_{sh,a}C_{d,a}\frac{C_{v,s}}{C_{a,s}}\frac{dX_{t,a}}{dt} \\ &\quad = C_{aoc}V_{t,c}P_{rs,o} + C_{cv}(X_{t,ss} - X_{t,a}) \\ &\qquad - C_{cn-cv}(X_{t,a} - P_{t,o}) - \frac{C_{d,a}C_{sh,a}}{C_{a,s}}\phi_v(X_{t,a} - P_{t,o}) \\ &\qquad - E_t(C_{et} - C_f X_{t,a}) \end{aligned} \quad (3)$$

where the ventilation flow is represented by:

$$\begin{aligned} \phi_v = \Bigg[&\left(\frac{V_{v,a-l}V_{v,a-r}}{\sqrt{V_{v,a-l}^2 + V_{v,a-r}^2}}\right)^2 \left(2C_g C_{ven,h}\frac{X_{t,a} - P_{t,o}}{X_{t,a} + P_{t,o}}\right) \\ &+ \left(\frac{V_{v,a-l} + V_{v,a-r}}{2}\right)^2 C_{ven,w}P_{ws,o}^2 \Bigg]^{0.5} C_{v,d} + \phi_l \end{aligned} \quad (4)$$

with

$$V_{v,a-l} = C_{v,l-l}C_{v,w-l}U_{ven}n_l \quad (5)$$

$$V_{v,a-r} = 2C_{v,l-r}C_{v,w-r}\sin\left(\frac{U_{ven}}{2}\right)n_r \quad (6)$$

and where the different coefficients and parameters are described in Table 1. Notice that crop evatranspiration, E_t, is evapotranspiration is obtained based on the crop state and climate variables as greenhouse air humidity and net radiation. The evaporation process in soil surface has been neglected due to the greenhouse is mulched [9].

On the other hand, U_{ven} is the vent opening (control signal) and represents the aperture value for both lateral and roof windows.

Thus, the model presented in (2) allows to describe the evolution of the diurnal greenhouse temperature (process output) based on the vent opening (control signal) and the process disturbances. Notice that this non-linear model has been calibrated and validated in previous works with a goodness of fit over 90% [8], [9].

In order to deal with the non-linearities of the model, the feedback linearization technique is used. The main idea behind this technique [10] is the treatment of non-linear systems as if they were linear, by means of algebraic transformations and feedback [17]. Equation (3) can be rewritten as follows:

$$\begin{aligned} A\frac{dX_{t,a}}{dt} + BX_{t,a} = {} & C_{aoc}V_{t,c}P_{rs,o} + C_{cv}X_{t,ss} \\ & + C_{cn-cv}P_{t,o} - \frac{C_{d,a}C_{sh,a}}{C_{a,s}}\phi_v(X_{t,a} - P_{t,o}) \\ & - E_t(C_{et} - C_f X_{t,a}) \end{aligned} \tag{7}$$

where

$$\begin{aligned} A &= C_{sh,a}C_{d,a}\frac{C_{v,s}}{C_{a,s}} \\ B &= C_{cv} + C_{cn-cv} \end{aligned}$$

Then, this model is transformed into canonical form (8) using functions g and b which depend on the system disturbances, $\varrho = (P_{rs,o}, X_{t,ss}, P_{t,o}, E_t)$:

$$\begin{aligned} \dot{x} &= g(x, \varrho) + b(x, \varrho) \cdot v \\ y &= h(x) \end{aligned} \tag{8}$$

where

$$x = X_{t,a} \tag{9}$$

$$g(x, \varrho) = -\frac{C_{a,s} \cdot (C_{cv} + C_{cn-cv}) \cdot x}{C_{sh,a}C_{d,a}C_{v,s}} \tag{10}$$

$$b(x, \varrho) = \frac{C_{a,s}}{C_{sh,a}C_{d,a}C_{v,s}} \tag{11}$$

$$\begin{aligned} v = {} & C_{aoc}V_{t,c}P_{rs,o} + C_{cv}X_{t,ss} + C_{cn-cv}P_{t,o} \\ & - \frac{C_{d,a}C_{sh,a}}{C_{a,s}}\phi_v(X_{t,a} - P_{t,o}) - E_t(C_{et} - C_f X_{t,a}) \end{aligned} \tag{12}$$

$$h(x) = x \tag{13}$$

Then, the following first-order input-output relationship is found:

$$\begin{aligned} A\dot{x} + Bx &= v \\ y &= x \end{aligned} \tag{14}$$

So, FL makes possible to use a linear controller to regulate the inside temperature $X_{t,a}$ by means of the virtual control signal $v(t)$ and according to (14). Then, once the virtual control signal is calculated, the real control signal U_{ven} is computed according to (4)-(6), and (12).

To account for the actuator saturation (the window opening is limited between 0° and 45°), a standard anti-reset wind-up mechanism [18] has been implemented. Since anti wind-up must be applied to the virtual signal, window opening limits are transformed into virtual signal limits using the inverse transformation of (12). Thus, in this case, the limits on the virtual control signal ($v_{min}(t)$ and $v_{max}(t)$) (see Figure 3) are computed from equations (6), (6) and (12). The maximum value of $v(t)$ is obtained when the variable U_{ven} has its minimum value, while the minimum value of $v(t)$ corresponds to the maximum value of U_{ven}, taking into account that U_{ven} varies between 0° and 45°.

In order to identify the characteristic parameters for the linear model, the FL block was implemented at the real plant input, and several open-loop step inputs were applied to the virtual control signal, $v(t)$. The open-loop tests were performed around noon and for 15 days with different disturbance profiles. Figure 4 shows an example of four open-loop tests, where different profiles of solar radiation and wind speed (the faster disturbances) are observed. Notice that the vent aperture and the temperature are shown in % and °C in all the figures for a better understanding. Figure 5 represents the first of these days. As it can be seen from the figure, an overdamped response was observed such as expected, and thus a FOPDT model was used to capture the process dynamics relating the greenhouse inside temperature, $X_{t,a}(t)$, with respect to the virtual control signal, $v(t)$. Figure 5 shows also a validation of the FOPDT model obtained for this day. Therefore, different FOPDT models were obtained for all the 15 open-loop tests, and it was observed that the FOPDT model parameters vary between a certain range, what results in the following uncertain model:

$$\begin{aligned} P(s) = \frac{X_{t,a}(s)}{V(s)} &= \frac{k}{\tau s + 1}e^{-ds} \\ k &\in [0.0021, 0.0084] \\ \tau &\in [9, 32]min \\ d &\in [2, 7]min \end{aligned} \tag{15}$$

Notice that this variation in the linear model parameters is because of the complexity of the process, the modelling error coming from the coefficients in the non-linear model (3), and the disturbance source. So, this uncertain model is used in the following section to design a robust PI to control the system.

B. QFT-BASED PI CONTROLLER

Due to the uncertainty in the system observed in the previous section, a robust control technique must be used. QFT methodology [19] is chosen for this purpose. The first step in QFT is to choose performance and stability specifications. Notice that the final control scheme is given by Figure 3.

Considering the uncertain model given by (15), and according to the magnitude of the time constant and the delay, the low frequency range is of interest in this case. Notice that in QFT, several frequency values must be selected for the controller design procedure. So, in this case, the following four

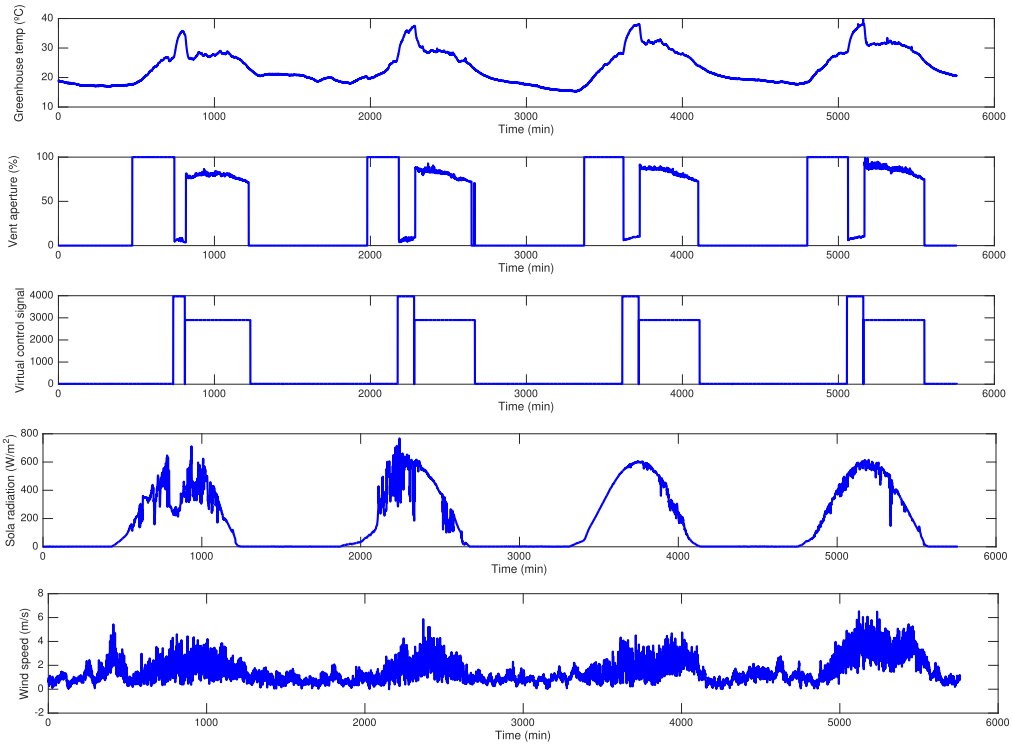

FIGURE 4. Open-loop tests with the feedback linearization block for 4 days.

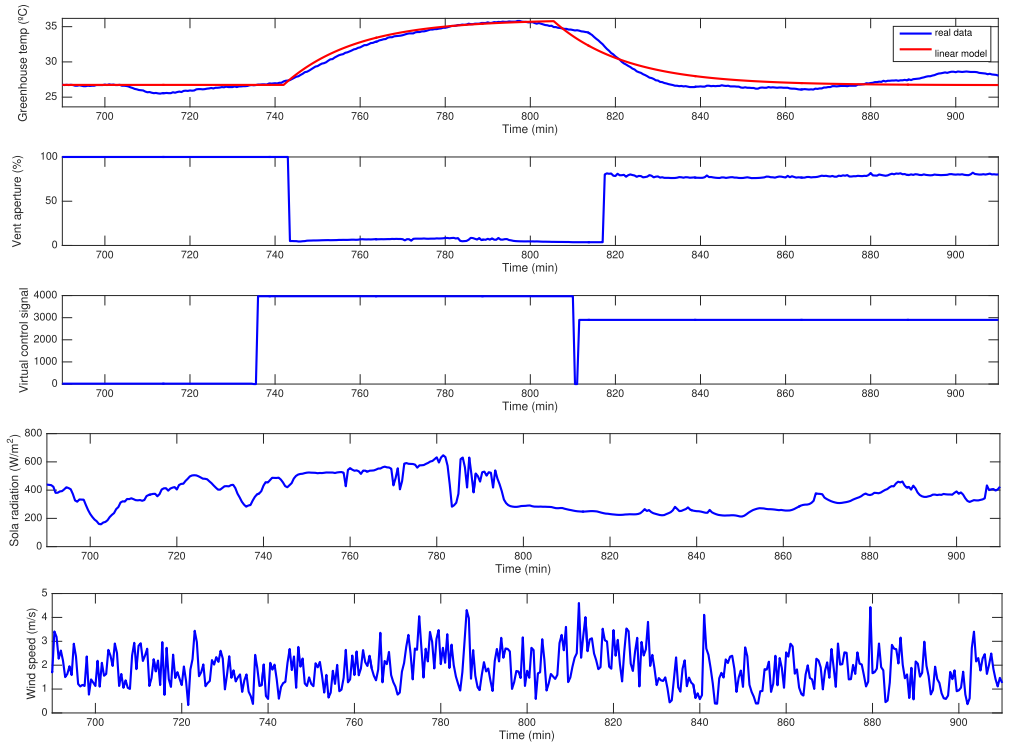

FIGURE 5. Greenhouse model validation for the first day in Figure 4.

representative values have been chosen to cover widely the low frequency range, $W = \{0.0001 0.005 0.01 0.1\}$ rps [20]. A specification of phase margin greater or equal to 45° for all plants is considered. Due to the nature of the system, the main objective to take into account is to look for a solution for the regulation problem. So, the following specification for input

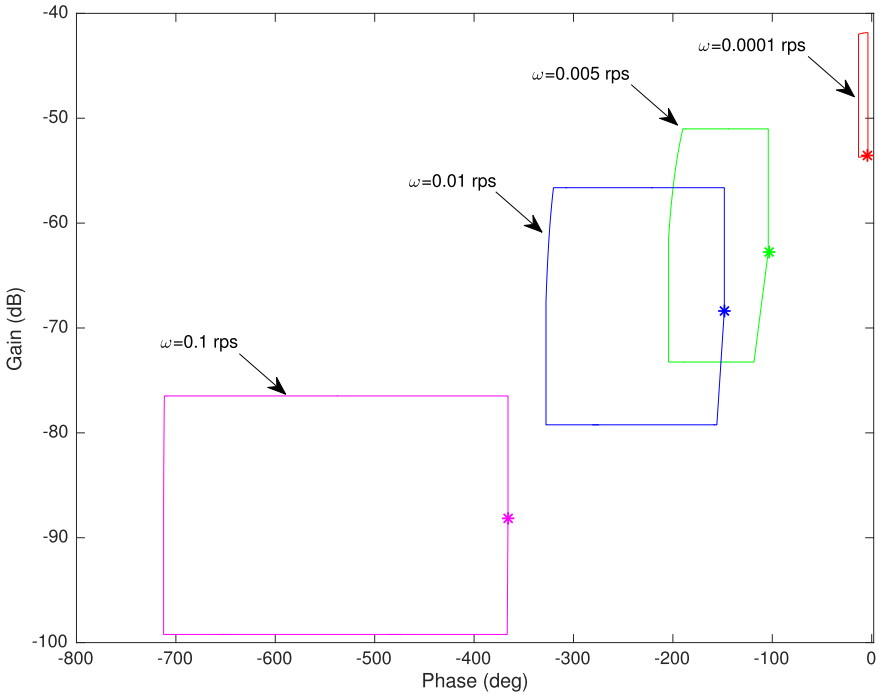

FIGURE 6. Templates for frequencies in W.

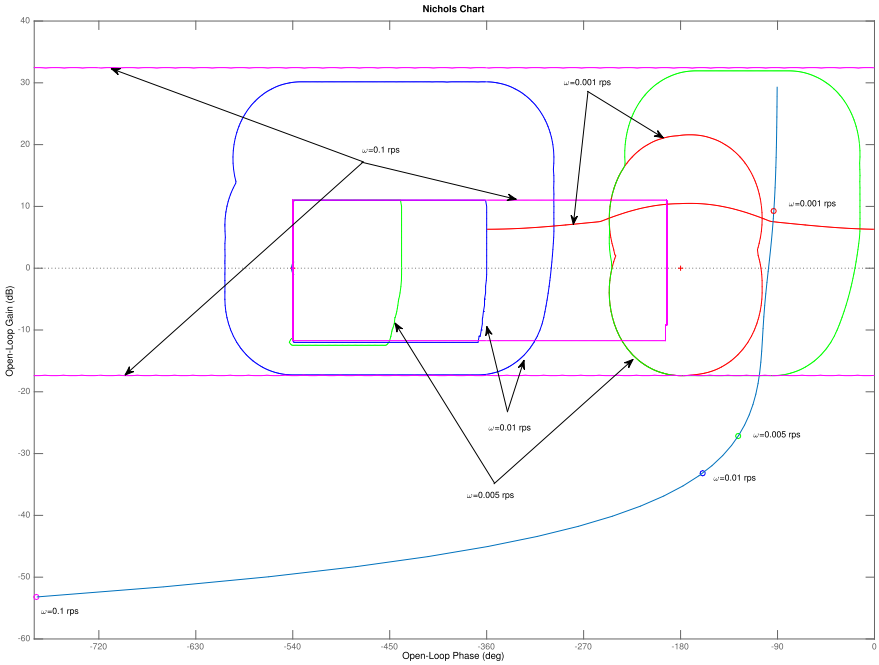

FIGURE 7. Stability and disturbances rejection bounds, and nominal open loop shaping.

disturbances rejection is considered

$$|T_{dy}(j\omega)| = \left|\frac{P(j\omega)}{1 + C(j\omega)P(j\omega)}\right| \leq \left|\frac{K_d j\omega}{(\tau_d j\omega + 1)^n}\right| \quad \forall \omega \in W \tag{16}$$

where $\tau_d = (0.95/n) * \tau_{ol}$, with $K = 9$, $n = 2$ and $\tau_{ol} = 9$ min. The parameter τ_{ol} is chosen as the open loop time constant for the slowest plant. The nominal plant chosen for design is given by $k = 0.0021$, $\tau = 32$ min, and $d = 2$ min.

In order to proceed with the design of the controller, the value sets or templates [21], which describe the system uncertainty in the Nichols Chart, are computed from Eq. (15) and the design frequencies set W, resulting in the representation showed in the Figure 6.

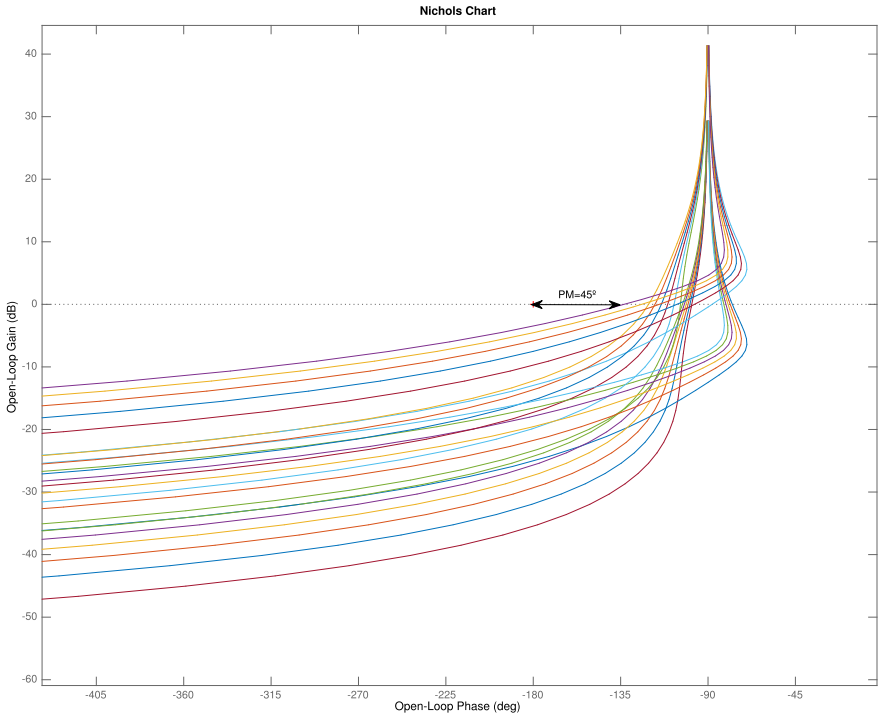

FIGURE 8. Validation for stability specification (phase margin of 45 degrees).

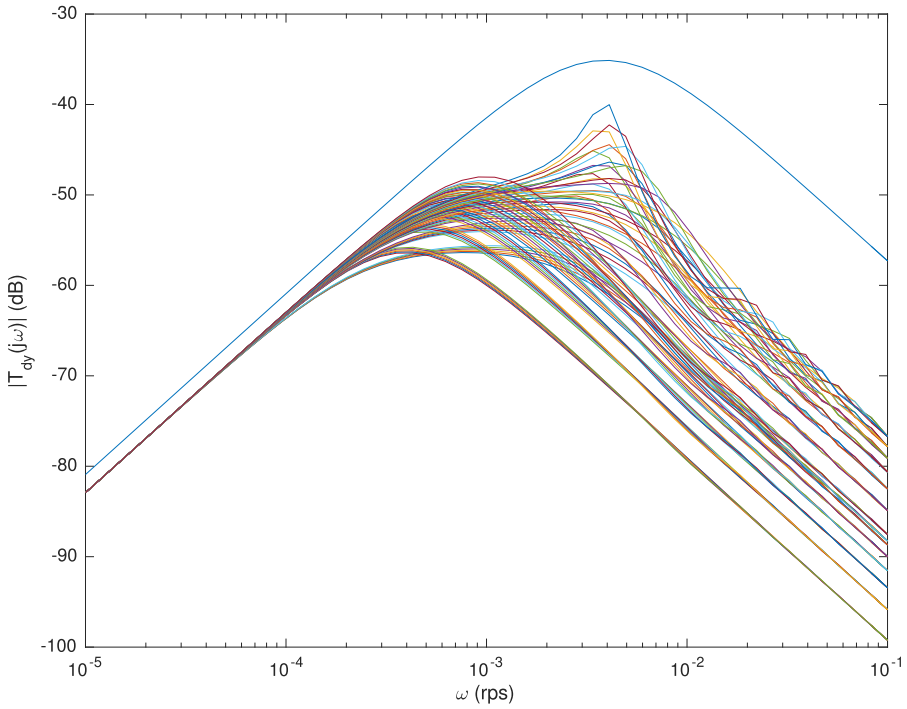

FIGURE 9. Validation for input disturbances rejection specification.

Using the algorithm in [22], the performance and stability boundaries are computed such as shown in Figure 7. Then, the nominal open loop transfer function is shaped to fulfill the required specifications [23]. Based on the resulting boundaries, a PI controller can be tuned to satisfy the specifications, resulting in the PI controller given by (17). Figure 7 shows the nominal open loop transfer function fulfilling all boundaries for frequencies in W.

$$C(s) = \frac{0.14(s/0.0007 + 1)}{s} \tag{17}$$

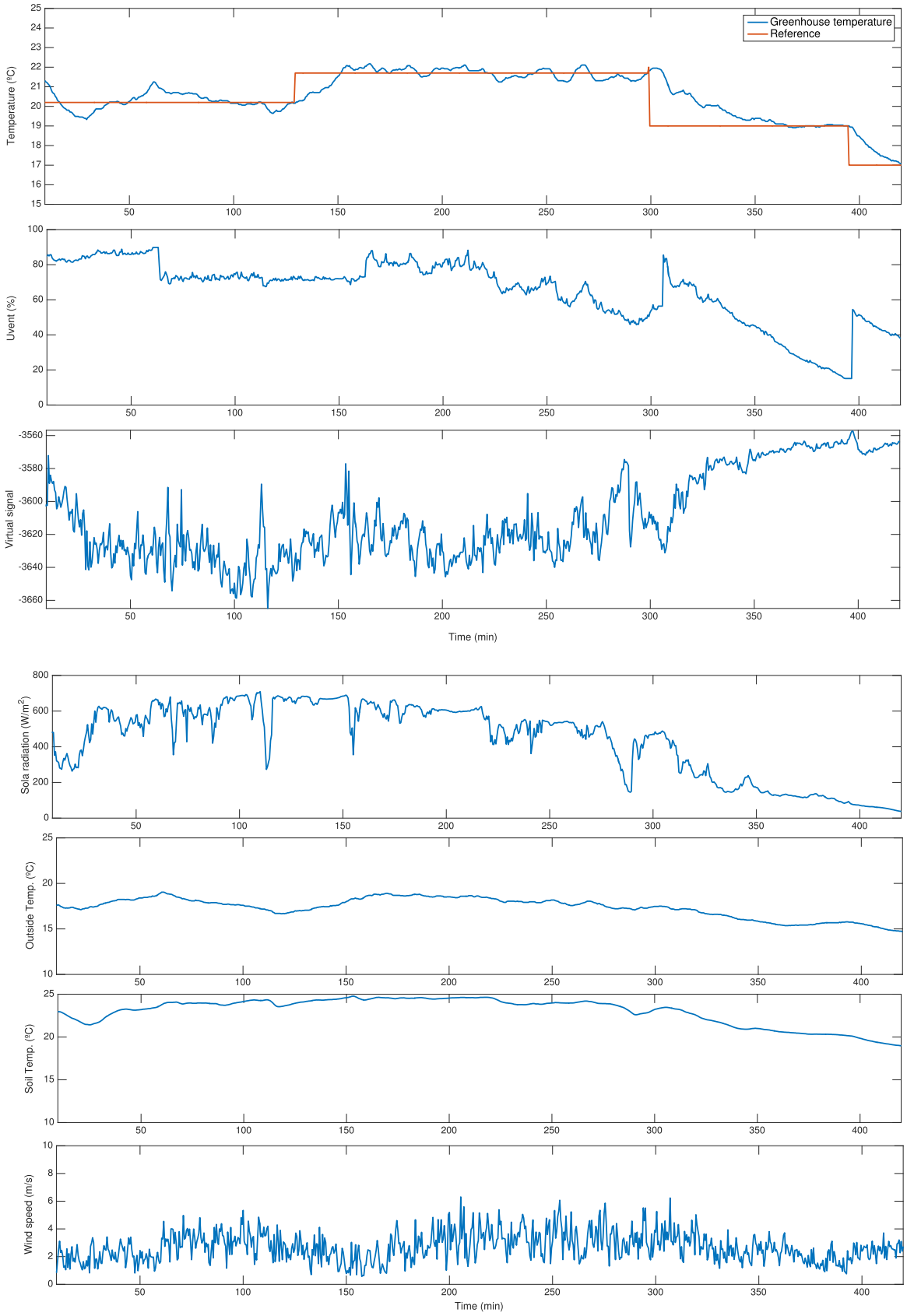

FIGURE 10. Control results for March 10th 2018. Figure at the top shows the process output and the control signals. Figure at the bottom represents the process disturbances: Solar radiation, outside temperature, soil temperature, and wind speed.

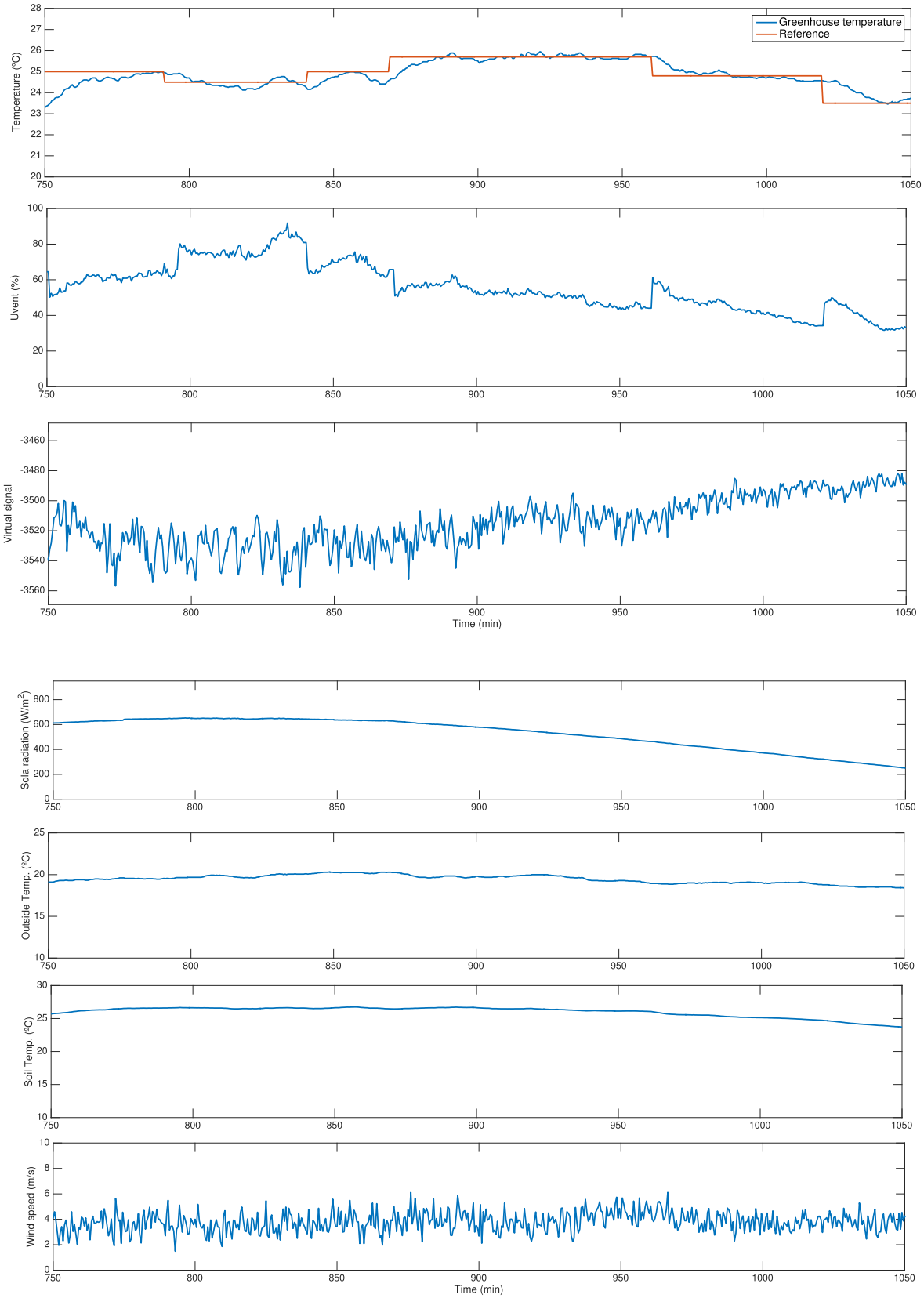

FIGURE 11. Control results for March 11th 2018. Figure at the top shows the process output and the control signals. Figure at the bottom represents the process disturbances: Solar radiation, outside temperature, soil temperature, and wind speed.

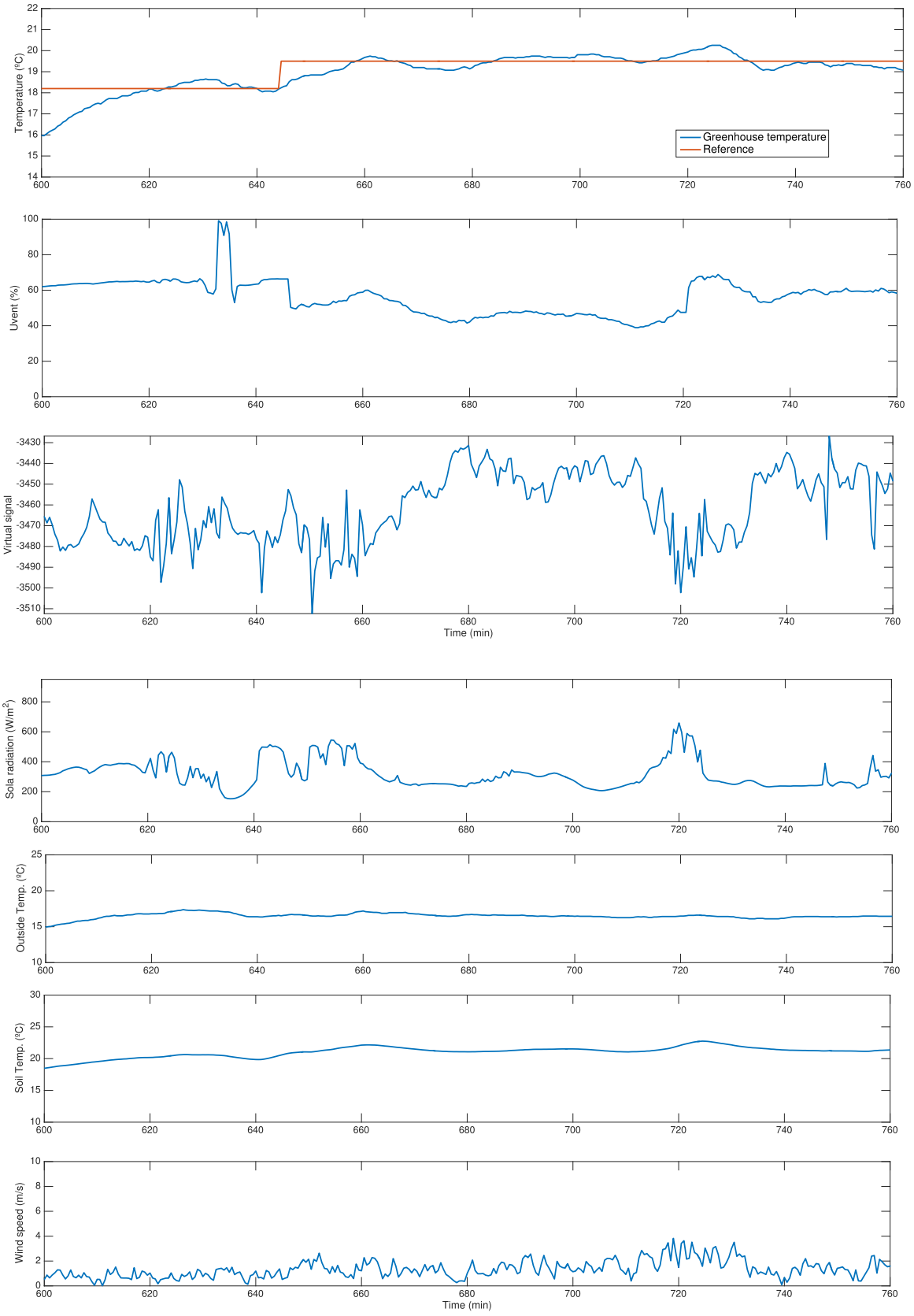

FIGURE 12. Control results for March 14th 2018. Figure at the top shows the process output and the control signals. Figure at the bottom represents the process disturbances: Solar radiation, outside temperature, soil temperature, and wind speed.

Figures 8 and 9 show the validation for the designed PI controller, where it is observed that all the specifications are satisfied.

Regarding the saturation problem, an anti-windup approach was used for the resulting PI controller, where the constraints in the vents were mapped to constraints in the virtual control signal such as described in Section III.A.

IV. EXPERIMENTAL RESULTS

In this section, some illustrative results performance at the real facilities are shown and discussed. Figures 10-12 show three different experimental tests for different weather and operating point conditions. The control signal, U_{ven}, is expressed in percentage for a clear understanding. Furthermore, in these experiments, different setpoint profiles are given to analyze the response of the proposed control approach. Figures 10(a) and (b) show the results for a cloudy day and with important variations in the wind speed. As observed from Figure 10(a), different step changes were performed for the inside temperature in order to show how the proposed control approach is able to follow the reference in spite of the disturbances variations. Moreover, from this figure, it is also observed how the virtual control signal is changing continuously to provide the adequate vent aperture in order to compensate the disturbance variations. Notice that the main changes on the virtual control signal are mainly due to solar radiation variations, as observed in time instants 115, 155 and 285 min. On the other hand, the virtual control signal presents a high variability due to the wind speed disturbance. However, this variability is compensated by the feedback linearization and thus it is not appearing on the vent aperture.

Figures 11(a) and (b) show a second example for a clear day, but with a constant wind speed of around 4 m/s. Figure 11(a) shows how both the virtual control signal and the vent aperture from the robust PI controller and the feedback linearization block respectively, softly vary in this case to keep the inside temperature close to the proposed reference. The higher changes in the ventilation control signal occur exactly where the changes on the temperature reference are applied. In the rest of the experiment, the ventilation aperture varies slowly due to soft variations in the system disturbances. However, it can be observed that from time instant 875 to the end of the experiment, the virtual control signal starts to increase to compensate the continuous decrease in the solar radiation. On the other hand, again, the variability in the wind speed is translated to the virtual control signal, but not to the ventilation aperture.

Finally, Figures 12(a) and (b) show a third example for a cloudy day with separated and intermittent passing clouds. Moreover, in this case, a slow wind speed was observed and for this reason, now the virtual control signal does not have too much variability. Figure 12(a) shows the control results where it is interesting to see how the virtual control signal and the vent aperture strongly vary around time instants $t = 620$ min and $t = 740$ min to compensate the strong radiation changes. Thus, it is again observed how the proposed control approach attenuates the effect of the disturbances on the ventilation aperture. Notice that this is an important advantage for the actuator lifetime.

So, notice how the proposed control approach is able to cope with the non-linear behavior of the system and the process variability due to an important changes in the operating point and process disturbances. The control scheme was able to keep the proposed setpoint values providing promising results for the greenhouse inside temperature control problem.

V. CONCLUSIONS

This paper has presented the combination of two control techniques in order to approach the diurnal greenhouse climate control problem. First, a feedback linearization control strategy has been implemented and tested in the plant. Despite cancelling the non-linearities of the model, discrepancies from the real system were observed being captured as parametric uncertainty. Then, a PI controller was designed using QFT and evaluated in the real system. The proposed control approach was tested in different days with different weather and operating conditions. The control system was able to reach the proposed setpoint changes in spite of the changes in the disturbances and in the operating points.

REFERENCES

[1] G. van Straten, G. van Willigenburg, E. van Henten, and R. van Ooteghem, *Optimal Control of Greenhouse Cultivation*. Boca Raton, FL, USA: CRC Press, 2010.

[2] C. Lijun, D. Shangfeng, H. Yaofeng, and L. Meihui, "Linear quadratic optimal control applied to the greenhouse temperature hierarchal system," in *Proc. 6th IFAC Conf. Bio-Robot.*, Beijing, China, 2018, pp. 712–717

[3] Q. Zou, J. Ji, S. Zhang, M. Shi, and Y. Luo, "Model predictive control based on particle swarm optimization of greenhouse climate for saving energy consumption," in *Proc. World Automat. Congr.*, Kobe, Japan, Sep. 2010, pp. 123–128.

[4] J. del Sagrado, J. A. Sánchez, F. Rodríguez, and M. Berenguel, "Bayesian networks for greenhouse temperature control," *J. Appl. Logic*, vol. 17, pp. 25–35, Sep. 2016.

[5] D. Xu, S. Du, and L. G. van Willigenburg, "Optimal control of Chinese solar greenhouse cultivation," *Biosyst. Eng.*, vol. 171, pp. 205–219, Jul. 2018.

[6] A. Pawlowski, M. Beschi, J. L. Guzmán, A. Visioli, M. Berenguel, and S. Dormido, "Application of SSOD-PI and PI-SSOD event-based controllers to greenhouse climatic control," *ISA Trans.*, vol. 65, pp. 525–536, Nov. 2016.

[7] J. K. Gruber, J. L. Guzmán, F. Rodríguez, C. Bordons, M. Berenguel, and J. A. Sánchez, "Nonlinear MPC based on a Volterra series model for greenhouse temperature control using natural ventilation," *Control Eng. Pract.*, vol. 19, no. 4, pp. 354–366, Apr. 2011.

[8] A. Ramírez-Arias, F. Rodríguez, J. L. Guzmán, and M. Berenguel, "Multiobjective hierarchical control architecture for greenhouse crop growth," *Automatica*, vol. 48, no. 3, pp. 490–498, 2012.

[9] F. Rodríguez, M. Berenguel, J. L. Guzmán, and A. Ramírez, *Modeling and Control of Greenhouse Crop Growth*. London, U.K.: Springer, 2015.

[10] M. A. Henson and D. E. Seborg, *Nonlinear Process Control*. Upper Saddle River, NJ, USA: Prentice-Hall, 1998.

[11] G. D. Pasgianos, K. G. Arvanitis, P. Polycarpou, and N. Sigrimis, "A nonlinear feedback technique for greenhouse environmental control," *Comput. Electron. Agricult.*, vol. 40, nos. 1–3, pp. 153–177, 2003.

[12] C. Lijun, D. Shangfeng, L. Meihui, and H. Yaofeng, "Adaptive feedback linearization-based predictive control for greenhouse temperature," in *Proc. 6th IFAC Conf. Bio-Robot.*, Beijing, China, 2018, pp. 784–789.

[13] S. Piñón, M. Peña, C. Soria, and B. Kuchen, "Nonlinear model predictive control via feedback linearization of a greenhouse," in *Proc. 4th IFAC Symp. Intell. Compon. Instrum. Control Appl.*, Buenos Aires, Argentina, 2000, pp. 191–196.
[14] J. C. Moreno, M. Berenguel, F. Rodríguez, and A. Baños, "Robust control of greenhouse climate exploiting measurable disturbances," in *Proc. 15th IFAC World*, Barcelona, Spain, 2002, pp. 271–276.
[15] G. P. A. Bot, "Greenhouse climate: From physical processes to a dynamic model," Ph.D. dissertation, Dept. Phys. Meteorol., Agricult. Univ. Wageningen, Wageningen, The Netherlands, 1983.
[16] E. J. Van Henten and J. Bontsema, "Time-scale decomposition of an optimal control problem in greenhouse climate management," *Control Eng. Pract.*, vol. 17, no. 1, pp. 88–96, Jan. 2009.
[17] J. D. J. Rubio, "Robust feedback linearization for nonlinear processes control," *ISA Trans.*, vol. 74, pp. 155–164, Mar. 2018.
[18] K. J. Astrom, *PID Controllers: Theory, Design and Tuning*. Pittsburgh, PA, USA: Instrument Society of America, 1995.
[19] I. Horowitz, *Quantitative Feedback Design Theory (QFT)*. Boulder, CO, USA: QFT Publications, 1993.
[20] J. L. Guzmán, J. C. Moreno, M. Berenguel, F. Rodríguez, and J. Sánchez-Hermosilla, "A frequency domain quantitative technique for robust control system design," in *Robust Control*, A. Bartoszewicz, Ed. Rijeka, Croatia: IntechOpen, 2011, ch. 17.
[21] B. R. Barmish, "New tools for robustness analysis," in *Proc. 27th IEEE Conf. Decis. Control*, Austin, TX, USA, vol. 1, 1988, pp. 1–6.
[22] J. C. Moreno, A. Baños, and M. Berenguel, "Improvements on the computation of boundaries in QFT," *Int. J. Robust Nonlinear Control*, vol. 16, no. 12, pp. 575–597, 2006.
[23] C. Borguesani, Y. Chait, and O. Yaniv, *The Quantitative Feedback Theory Toolbox for MATLAB*. Natick, MA, USA: The MathWorks, 1995.

A. HOYO received the degree in electronic engineering and the master's degree in industrial engineering from the University of Almería, Spain, in 2016 and 2018, respectively. She is currently pursuing the Ph.D. degree in non-linear and robust control techniques. She is currently a Researcher with the Automatic Control, Robotic, and Mechatronic Group, University of Almería.

J. C. MORENO received the M.Sc. degree (Hons.) in computer science engineering and the Ph.D. degree from the University of Murcia, in 1996 and 2003, respectively. Since 1999, he has been a Professor system engineering and automatic control with the Department of Computer Science, University of Almería. He performs teaching tasks related to automatic control and robotics. He is also a Researcher and a member of the Automatic Control, Mechatronics and Robotics Research Group. His current research interests are automatic control theory and robotics and their application to energetic, biological, and industrial environments.

J. L. GUZMÁN received the M.Sc. degree in computer science engineering and the Ph.D. degree (Hons.) from the University of Almería, Almería, Spain, in 2002 and 2006, respectively. He is currently a Full Professor of automatic control and systems engineering with the University of Almería. His current research interests include MPC techniques, PID control, and robust control with applications to agricultural processes, solar plants, and biotechnology. He has been a member of the Spanish IFAC Association of Automatic Control, since 2003 and of the IEEE Control Systems Society, since 2006, the IFAC Technical Committee on Control Education, and the IEEE Technical Committee on System Identification and Adaptive Control, since 2008.

F. RODRÍGUEZ received the M.Sc. degree in telecommunication engineering from the Universidad Politécnica de Madrid, Madrid, Spain, and the Ph.D. degree from the University of Almería, Almería, Spain, in 2002. He is currently a Full Professor of systems engineering and automatic control with the University of Almería, where he is also a Researcher and a member of the Automatic Control, Mechatronics and Robotics Research Group. He has participated in several Spanish and European research projects, research, and development tasks with many companies. His current research interests include the application of modelling, automatic control, and robotics techniques to dynamic systems and education, concretely energy management, and agriculture. He has been a member of the IFAC Technical Committee TC 8.1, Control in Agriculture, since 2005.